Sheath structure for cylindrical probe in low-pressure electronegative discharges

T. H. Chung
Department of Physics, Dong-A University, Busan 604-714, Korea

(Received 11 October 2005; accepted 18 January 2006; published online 16 February 2006)

A theoretical model for collisionless and weakly collisional plasmas with cold positive ions is developed for the presheath and sheath that surround a cylindrical probe immersed in electronegative discharges. The model is solved numerically, and the spatial distributions of the normalized potential, the normalized density, and the normalized velocity and flux of positive ions are calculated for a low-pressure electronegative discharge as a function of the ratio of the negative ion density to the electron density and the ratio of the electron temperature to the negative ion temperature. As the ratio of the Debye length to the ionization length increases, it is found that the sheath width decreases, the velocity of the positive ion gets smaller, and the positive ion flux to the probe decreases. As the electronegativity increases, the sheath width decreases. © *2006 American Institute of Physics*. [DOI: 10.1063/1.2172934]

Negative ions are found in electronegative gases such as oxygen, chlorine, SF_6, and fluorocarbons, which are used extensively in discharges for various applications of plasma processing. The presence of negative ions complicates the discharge phenomena. There has been an increased demand to determine the plasma parameters such as charged particle densities, sheath width, electron temperature, and plasma potential for electronegative plasmas.

In previous papers,[1–3] plasma parameters for electronegative discharges were obtained from the standard Langmuir probe method. We explored the scaling relations and observed that the experimentally measured scalings of the charged species are in agreement with the predictions of the spatially averaged global model.[4] However, in those studies, we estimated the positive ion density directly from the positive ion saturation current assuming that the positive ions have the normal Bohm velocity, which is not accurate.

The presence of the negative ions complicate the characteristics of the probe *I-V* curve. The negative ions begins to contribute to the probe current near the plasma potential, and the amount of the contribution gets larger when the probe voltage approaches the plasma potential. The ion saturation zone of the *I-V* characteristics of the probe is increasingly used in plasma diagnosis.[5] The current drained by the probe in this zone is very small and reduces the perturbation that the measurement causes in the plasma. The sheath structure and the motion of positive ions within the presheath and sheath are modified when negative ions are present. The precise values of positive ion density and ion velocity at the sheath edge should be formulated.

The main issue lies in the modeling of the positive ion flux to the probe for electronegative plasmas. In this study, the positive ions are modeled as a cold, collisionless, or weakly collisional fluid, while both the electron and negative ion densities obey Boltzmann relations. The positive ion flux is calculated along the distance from the plasma bulk region to any arbitrarily small distance near the probe edge using a set of coupled equations including the steady-state fluid equations of continuity and motion for the positive ion, the Poisson equation with Boltzmann electron, and the Boltzmann negative ion.[6,7] The equations are one-dimensional assuming no orbital motion of the positive ions. The positive ions are all drawn radially into the probe. This theoretical model of the positive ion flux for cylindrical and spherical probes has been developed by several researchers.[6–8]

For simplicity, we consider that electronegative plasma consists of three charged species, which are positive ion, negative ion, and electron. The ion continuity and momentum balance equations are

$$\nabla \cdot [n_+ \mathbf{v}_+] = \nu_{iz} n_e, \tag{1}$$

$$\nabla \cdot [n_+ \mathbf{v}_+ \mathbf{v}_+] = e n_+ \mathbf{E}, \tag{2}$$

where n_+ is the positive ion density, $\mathbf{v}_+$ is the velocity of positive ion, n_e is the electron density, ν_{iz} is the ionization frequency, and $\mathbf{E}$ is the electric field.

We assume that electrons and negative ions follow the Boltzmann energy distribution,

$$n_e = n_{e0} \exp\left(\frac{eV}{kT_e}\right), \tag{3}$$

$$n_- = n_{-0} \exp\left(\frac{eV}{kT_-}\right), \tag{4}$$

where n_- is the negative ion density, T_e and T_- are the temperature of the electrons and negative ions, e is the electron charge, k is the Boltzmann constant, and V is the electric potential. The subscript 0 indicates the value at the plasma bulk region.

Poisson's equation is written as

$$\varepsilon_0 \nabla \cdot \mathbf{E} = e(n_+ - n_e - n_-), \quad \mathbf{E} = -\nabla V, \tag{5}$$

where ε_0 is the permittivity of the vacuum.

The model equations are developed for cylindrical electrode (probe) sheaths with radial motion of positive ions toward the probe. We have the dimensionless functions and parameters;

$$\xi = \frac{r}{\lambda_D}, \quad \tilde{n} = \frac{n_+}{n_{+0}}, \quad u = \frac{v_+}{c_s}, \quad \eta = -\frac{eV}{kT_e},$$

$$\alpha_0 = \frac{n_{-0}}{n_{e0}}, \quad \gamma = \frac{T_e}{T_-}, \tag{6}$$

where c_s is the Bohm velocity ($=kT_e/m_+$; m_+ is the ion mass), and λ_D is the Debye length.

The nondimensionalized equations of ion continuity and momentum balance for positive ion, and Poisson's equation in cylindrical coordinate, are written

$$\frac{d}{d\xi}(\tilde{n}u) + \frac{\tilde{n}u}{\xi} = \frac{q}{1+\alpha_0} e^{-\eta}, \tag{7}$$

$$\frac{d}{d\xi}(\tilde{n}uu) + \frac{\tilde{n}uu}{\xi} = \tilde{n}\varepsilon, \tag{8}$$

$$\frac{d\varepsilon}{d\xi} + \frac{\varepsilon}{\xi} = \tilde{n}(1+\alpha_0) - e^{-\eta} - \alpha_0 e^{-\gamma\eta}, \tag{9}$$

$$\frac{d\eta}{d\xi} = \varepsilon, \tag{10}$$

where $q=\lambda_D/\Lambda$ is the non-neutrality parameter, and $\Lambda = c_s/\nu_{iz}$ is the ionization length.

In the presheath region, the space charge is very small and the potential variation may be derived from the quasineutral condition. Equating the right-hand side of Eq. (9) to zero, we have

$$\tilde{n}(1+\alpha_0) - e^{-\eta} - \alpha_0 e^{-\gamma\eta} = 0. \tag{11}$$

If we consider collisionless plasma with cold positive ions and assume no orbital motion

$$\tfrac{1}{2} m_+ v_+^2(r) + eV(r) = 0, \tag{12}$$

we have

$$a = \sqrt{2}\xi\tilde{n}\sqrt{\eta}, \tag{13}$$

where

$$a = \frac{j_D}{en_{+0}c_s}, \quad j_D = \frac{I_+}{2\pi\lambda_D}. \tag{14}$$

Here, $I_+ = 2\pi e r n_+ v_+$ is the positive ion current to the cylindrical probe per unit length. Equation (11) combined with Eq. (13) gives η as a function of ξ implicitly.

Differentiating Eq. (11) with respect to ξ and using Eq. (13), we obtain

$$\frac{d\eta}{d\xi} = \frac{-2\eta[1+\alpha_0 e^{-(\gamma-1)\eta}]}{\xi[(1+\alpha_0 e^{-(\gamma-1)\eta}) - 2\eta(1+\gamma\alpha_0 e^{-(\gamma-1)\eta})]}. \tag{15}$$

At the point where $d\eta/d\xi$ becomes infinite, the quasineutral condition fails and the space charge begins to develop. At this point η must satisfy

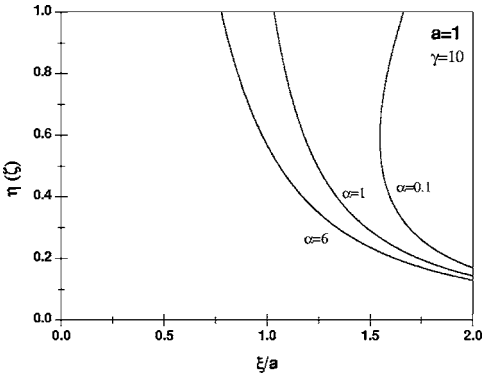

FIG. 1. Plasma solution for $a=1$, $\gamma=10$ for some values of α_0. Quasineutral presheath potentials are obtained by Eqs. (11) and (13).

$$\eta = \frac{1+\alpha_0 e^{-(\gamma-1)\eta}}{2(1+\gamma\alpha_0 e^{-(\gamma-1)\eta})}. \tag{16}$$

The sheath edge potential for the cylindrical probe has the same form as that in a planar and spherical probe.[6,7,9] In planar and spherical geometry electrodes, a collisionless plasma model with cold positive ions suggests that there are multiple solutions of the value of the sheath edge potential and an oscillatory potential structure is formed for certain values of α_0 and γ.[9,10] Like in spherical or planar geometry, there are multiple solutions for the presheath potential in cylindrical geometry. In Fig. 1, the quasineutral presheath potentials obtained by Eqs. (11) and (13) are shown for $a=1$, $\gamma=10$ for some values of α_0. It should be noted that Eqs. (11) and (13) are valid for the collisionless presheath region. The electric potential in the presheath region decreases when the negative ion concentration is increased. As the electronegativity α_0 increases, the sheath width is found to decrease. For the large α_0 case where the electron density is much less than the negative ion density, the sheath edge moves closer to the probe. As the negative ion density ratio is increased, both groups of negative particles compensate the presence of positive ions, causing a small net charge density and a decrease in potential.[8]

Figure 2 shows the relation between η and ξ given by Eqs. (11) and (13) for various values of a. The electric potential at sheath edge increases smoothly with increasing a.

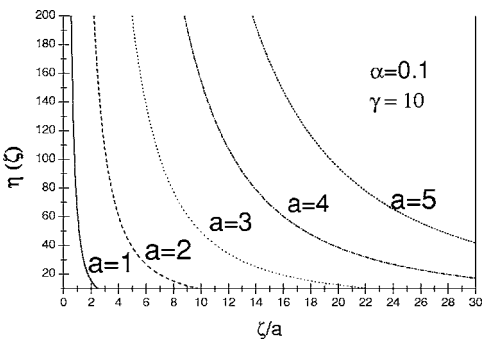

FIG. 2. Potential variations given by Eqs. (11) and (13) for various values of a. Here $\alpha_0=0.1$, $\gamma=10$.

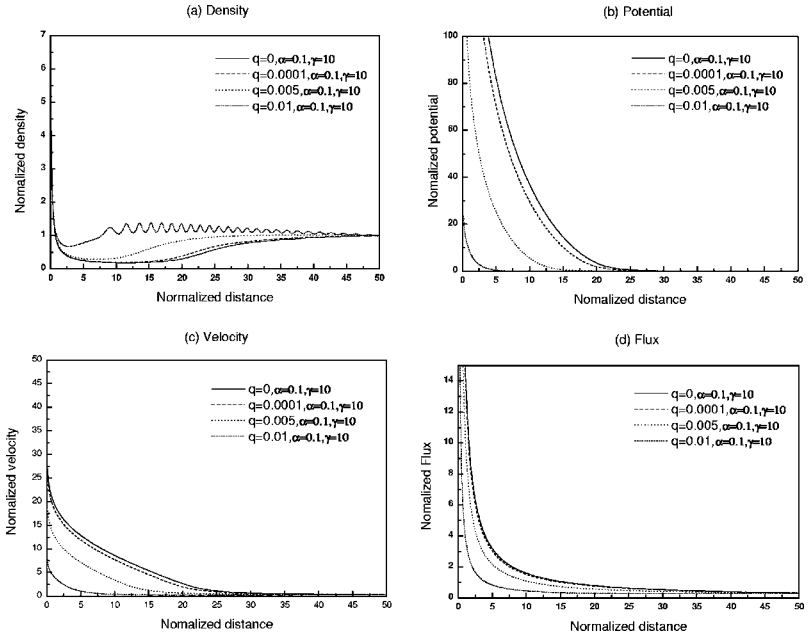

FIG. 3. Spatial distribution of (a) the positive ion density, (b) the electric potential, (c) the positive ion velocity, and (d) the positive ion flux around the cylindrical probe with various values of q. Here $\alpha_0=0.1$, $\gamma=10$.

Larger a results in larger positive ion current toward the probe, thus increasing the electric potential at each point.

The model equations (7)–(10) are solved numerically by using the fourth-order Runge-Kutta method with the initial values $\tilde{n}=1$, $u=0$, $\eta=0$, $\varepsilon=0$, at $\xi=\infty$, and the spatial distributions of the normalized potential, the normalized density, and the normalized velocity and flux of positive ions are obtained for a low-pressure, cylindrical, electronegative discharge as functions of the ratio (q) of the Debye length to the ionization length, the ratio (α_0) of the negative ion density to the electron density, and the ratio (γ) of the electron temperature to the negative ion temperature. Figures 3 and 4 are the results of this calculation.

Figure 3(a) shows the density profiles of positive ions at various values of q. The electric potential corresponding to the four different values of q is shown in Fig. 3(b). As q increases, the sheath width is found to decrease. This is due to the fact that the frequent ionization supplies the positive ions and electrons, thus the quasineutrality condition is achieved up to near the probe surface. However, as shown in Figs. 3(c) and 3(d), as q increases, the velocity of the positive ion gets smaller, and the positive ion flux to the probe decreases. As an example of the electronegative plasma, we can consider an oxygen discharge with $p=1$ mTorr, $T_e=2.6$ eV, $n_e=5.6\times10^{11}$ cm^{-3}. We have $\lambda_D=0.0015$ cm and $c_s=2.5\times10^5$ cm/s, $\nu_{iz}=10^61/\mathrm{s}$, $\Lambda=0.25$ cm, and $q=0.0063$. If we increase the gas pressure, we have higher q values. As the pressure increases, the ionization length decreases and thus q becomes large. When strict charge neutrality is relaxed as in the $q=0.001$ case, spatially oscillatory

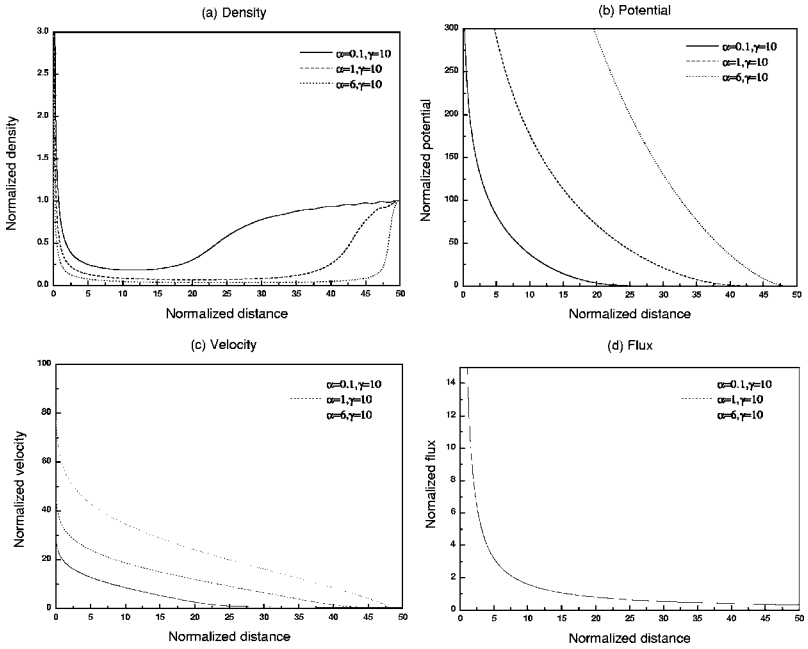

FIG. 4. Spatial distribution of (a) the positive ion density, (b) the electric potential, (c) the positive ion velocity, and (d) the positive ion flux around the cylindrical probe with various values of α_0. Here $q=0$, $\gamma=10$.

charge-density profiles are observed at the presheath region. Franklin and Snell have shown that the positive ion thermal motion, which takes place in real plasmas, affects the oscillatory structure and reduces the oscillations.[11,12] The oscillations arise from the unphysical assumption that the positive ion temperature is zero.

Figure 4(a) shows the density profiles of positive ions at various values of α_0. It is observed that the sheath edge expands as α_0 increases. The electric potential corresponding to the three different values of α_0 is shown in Fig. 4(b). In this case, the scales of the electric potential and distance are extended to larger values compared to Fig. 1. As α_0 increases, the potential increases to higher values and ξ extends to larger values than those for the case of $\alpha_0=0$. This means that the sheath width expands as α_0 increases. This result is in contradiction to the results of Crespo *et al.*,[8] but in agreement with the results of Amemiya *et al.*[13] However, the sheath edge should be defined as the point where the quasineutrality condition breaks down. As far as the sheath edge condition is concerned, Eqs. (11) and (13) should be used for small scale of the electric potential. Therefore, it can be stated that as the electronegativity α_0 increases, the sheath width decreases as shown in Fig. 1. As shown in Figs. 4(c) and 4(d), as α_0 increases, the velocity of the positive ion gets larger, and the positive ion flux to the probe remains the same because we assume no collision in this case.

This model allows us to obtain the *I-V* characteristic curve of the probe. The positive ion current to the probe is written as

$$I_+ = eS\Gamma_s(\alpha_0, \gamma, n_e), \tag{17}$$

where S is the probe area, $\Gamma_s(\alpha_0, \gamma, n_e)=n_{+s}v_{+s}$ is the modified Bohm flux, and n_{+s} and v_{+s} are the density and velocity of positive ions at sheath edge when negative ions are present.[7,14] Especially, in this model, the *I-V* characteristic curves of a cylindrical Langmuir probe can be obtained and compared with the experimental curve, which can give the estimation of α_0, γ and the electron density.[5] The theoretical *I-V* curve can be drawn in terms of the normalized parameters η and $I(=a\xi_p)$ (r_p is the radius of the probe). The parameter a depends on ξ_p, which in turn depends on the electron density to be determined.

For each assumed value of I (normalized probe current), the set of equations including Poisson's equation can be integrated from $\xi=\infty$ to any arbitrarily small ξ. The point on the curve where $\xi=\xi_p$ gives the normalized potential η_p for that value of I. By computing a family of curves for different I, one can obtain an I-η_p curve for a probe of radius ξ_p. From a selected values of I and η_p on the measured probe characteristics, we have to estimate ξ_p. The electron temperature is supposed to be determined from measuring the slope of the probe *I-V* curve. Then it is possible to determine the electron density, α_0, and γ. Using a density balance between negatively and positively charged particles given by $n_e+n_-=n_+$, we can estimate the positive ion density.[15]

In conclusion, a theoretical model is developed for the presheath and sheath region that surround the cylindrical Langmuir probe immersed in electronegative discharges. The spatial distributions of the normalized potential, the normalized density, and the normalized velocity and flux of positive ions are obtained. As the q increases, the sheath width decreases, the velocity of the positive ion gets smaller, and the positive ion flux to the probe decreases. As the electronegativity α_0 increases, the sheath width decreases.

ACKNOWLEDGMENTS

We are grateful to Professor A. J. Lichtenberg and Professor M. A. Lieberman of the University of California at Berkeley for fruitful discussions.

This work is supported by the Plasma Fusion User Program of Korea Basic Science Institute (the program year of 2005).

[1] T. H. Chung, H. J. Yoon, and D. C. Seo, J. Appl. Phys. **86**, 3536 (1999).
[2] T. H. Chung, D. C. Seo, G. H. Kim, and J. S. Kim, IEEE Trans. Plasma Sci. **29**, 970 (2001).
[3] D. C. Seo, T. H. Chung, H. J. Yoon, and G. H. Kim, J. Appl. Phys. **89**, 4218 (2001).
[4] C. Lee and M. A. Lieberman, J. Vac. Sci. Technol. A **13**, 368 (1995).
[5] R. Morales Crespo, J. I. Fernandez Palop, M. A. Hernandez, and J. Ballesteros, J. Appl. Phys. **95**, 2982 (2004).
[6] R. N. Franklin, Plasma Sources Sci. Technol. **9**, 191 (2000).
[7] T. E. Sheridan, P. Chabert, and R. W. Boswell, Plasma Sources Sci. Technol. **8**, 457 (1999).
[8] R. Morales Crespo, J. I. Fernandez Palop, M. A. Hernandez, S. Borrego del Pino, and J. Ballesteros, J. Appl. Phys. **96**, 4777 (2004).
[9] A. Kono, J. Phys. D **32**, 1357 (1999).
[10] A. Kono, J. Phys. D **34**, 1083 (2001).
[11] R. N. Franklin and J. Snell, J. Phys. D **23**, 1990 (2000).
[12] J. I. Fernandez Palop, J. Ballesteros, M. A. Hernandez, R. Morales Crespo, and S. Borrego del Pino, J. Phys. D **38**, 868 (2005).
[13] H. Amemiya, B. M. Annaratone, and J. E. Allen, Plasma Sources Sci. Technol. **8**, 179 (1999).
[14] P. Chabert, T. E. Sheridan, R. W. Boswell, and J. Perrins, Plasma Sources Sci. Technol. **8**, 561 (1999).
[15] H. Amemiya, J. Phys. D **23**, 999 (1990).